Progress of Theoretical Physics, Vol. 58, No. 4, October 1977

Basic Properties of a Stationary Accretion Disk Surrounding a Black Hole

Reiun HŌSHI

Department of Physics, Rikkyo University
Nishi-Ikebukuro, Tokyo

(Received June 17, 1977)

The structure of a stationary accretion disk surrounding a black hole is studied by means of newly developed basic equations. The basic equations are derived under the assumption that the vertical distribution of disk matter is given by a polytrope. For a Keplerian accretion disk, basic equations reduce to a differential equation of the first order. We have found that solutions of an optically thick accretion disk converge to a limiting value, irrespective of the outer boundary condition. This gives the happy consequence that the inner structure of an optically thick accretion disk is determined irrespective of the outer boundary condition. On the contrary, an optically thin accretion disk shows bimodal behavior, that is, two physically distinct states exist depending on the outer boundary condition imposed at the outer edge of the accretion disk.

§ 1. Introduction

Following the pioneer work by Pringle and Rees,[1] and Shakura and Sunyaev,[2] a number of theories[3),4)] based on a standard accretion disk model have been developed to account for X-ray observations of Cyg X-1. The standard treatment assumes viscous stress to be proportional to the gas or the radiation pressure, i.e., $P_{r\varphi}=-\alpha P_g$ or $-\alpha P_r$ (called the α-model). Recently, Ichimaru[5] has developed a theory of magneto-hydrodynamic turbulence and has formulated viscous stress arising from turbulent magnetic fields which are generated by differential rotation of disk matter. In particular, the new formulation reduces to the α-model if the gas pressure dominates the radiation pressure. The α-parameter determined from the new formulation is about 2/3.

The radial structure of a stationary accretion disk is governed by five basic equations that describe conservation laws of mass, momentum (radial, azimuthal and vertical components) and energy, respectively. In the standard treatment these equations, except for the momentum equation of the vertical component which describes vertical hydrostatic balance, are usually simplified by integrating the equations over the vertical coordinate. Integrations are sometimes replaced by (corresponding mean value $\times$ thickness of the disk), which gives rise to unnecessary uncertainties in the basic equations. In order to get rid of those uncertainties we introduce a concept of polytrope about the vertical distribution of accretion disk matter. With the aid of the polytrope we formulate the basic equations that are free from uncertainties arising from the above integrations.

The standard accretion disk model assumes Keplerian motion for accretion disk matter. Furthermore, the change of the internal energy and work done by pressure are ignored in the energy equation. In §§ 3~5, we examine the behavior of the terms neglected in the standard accretion model. If we assume a Keplerian accretion disk, basic equations reduce to a differential equation of the first order. We have found that solutions of an optically thick accretion disk, when numerical calculation is carried out inward from the outer edge of the disk, have converged to a limiting value, irrespective of the boundary condition. It is also shown that the result due to the standard model calculation coincides with the above limiting value. If the disk is geometrically thick, however, our limiting value differs from the standard model calculation.

It is of special interest to apply our theory to an optically thin accretion disk. As has been shown by Ichimaru,[6] an optically thin accretion disk shows bimodal behavior as will be discussed in § 5. When the physical condition of accreting matter near the outer edge of the disk crosses over a critical condition, a transition from one to other takes place. This bimodal behavior may play an important role to account for observations of galactic X-ray sources. However, in the present paper no implication between our theory and observations has been made, which will be discussed in near future.

§ 2. Basic equations

This chapter is devoted to the derivation of a set of basic equations that governs the radial structure of a stationary accretion disk. This can be achieved when the vertical structure of the accretion disk has been solved beforehand. However, the complete determination of the vertical structure requires knowledge about vertical energy flow as a function of the vertical coordinate. In order to derive the energy flow, both radial and vertical structures must be solved simultaneously. These complications can be bypassed when we assume a polytropic relation connecting pressure and density in place of the exact vertical distribution of accretion disk matter.

To describe an axisymmetric disk configuration of accretion matter, we employ a cylindrical system of coordinate (r, φ, z) with the z-axis chosen as the axis of rotation. Hydrostatic balance of one gram of disk matter at a radial distance r from the center and at a vertical distance z from the equatorial plane is given by

$$\frac{dP}{dz}=-\frac{GM}{r^2}\frac{z}{r}\rho\,, \tag{1}$$

where P and ρ are the pressure and density, and M the mass of the central star. In deriving Eq. (1) the z-component of gravity due to the central star has been approximated by GMz/r^3. The solution of Eq. (1) is given by

$$K(1+N)\rho^{1/N}=\frac{1}{2}\frac{GM}{r}\left\{\left(\frac{z_0}{r}\right)^2-\left(\frac{z}{r}\right)^2\right\}, \tag{2}$$

where we have used the polytropic relation given by $P=K\rho^{1+1/N}$ and z_0 is the thickness of the disk from the equatorial plane to the surface. Here, the surface of the disk is defined as a plane at which both the pressure and density reduce asymptotically to zero. Introducing non-dimensional variables

$$\sigma=\rho/\rho_0\,,\quad \xi=z/z_0\,, \tag{3}$$

we have from Eq. (2),

$$\sigma=(1-\xi^2)^N\,, \tag{4}$$

and at the equatorial plane we have

$$K(1+N)\rho_0^{1/N}=(1+N)\frac{P_0}{\rho_0}=\frac{GM}{2r}\left(\frac{z_0}{r}\right)^2, \tag{5}$$

where P_0 and ρ_0 are the pressure and density at the equatorial plane respectively. In terms of Eq. (4) one can integrate the density, pressure, viscous stress $P_{r\varphi}$ and energy loss rate ε_R over the vertical coordinate z,

$$\begin{aligned} S&=\int_{-z_0}^{z_0}\rho\,dz=2\rho_0 z_0 I(N)\,,\\ W&=\int_{-z_0}^{z_0}P\,dz=2P_0 z_0 I(N+1)\,, \\ &\left.\begin{aligned} W_{r\varphi}&=\int_{-z_0}^{z_0}P_{r\varphi}dz\,,\\ E_R&=\int_{-z_0}^{z_0}\varepsilon_R\,dz\,, \end{aligned}\right\} \quad \text{(Explicit expressions will be given later.)} \end{aligned} \tag{6}$$

where

$$I(N)=\frac{(2^N N!)^2}{(2N+1)!}\,. \tag{7}$$

In terms of Eq. (6) we can write down a set of basic equations which governs the radial structure of the accretion disk. Conservation laws of mass, angular momentum and energy read

$$2\pi r v_r S=\dot{M}\,, \tag{8}$$

$$S\left(v_r\frac{dv_r}{dr}-\frac{v_\varphi^2}{r}\right)=-\frac{GM}{r^2}S-\frac{dW}{dr}\,, \tag{9}$$

$$S\left(v_r\frac{dv_\varphi}{dr}+v_r\frac{v_\varphi}{r}\right)=-\frac{1}{r^2}\frac{d}{dr}(r^2W_{r\varphi})\,, \tag{10}$$

$$\frac{d}{dr}\left[\dot{M}\left(\frac{\gamma}{\gamma-1}\frac{W}{S}+\frac{1}{2}v_r^2+\frac{1}{2}v_\varphi^2-\frac{GM}{r}\right)+2\pi r^2W_{r\varphi}\Omega\right]-2\pi rE_R=0\,, \tag{11}$$

where $\dot{M}$ is the accretion rate, v_r the inward radial velocity, v_φ the azimuthal velocity, Ω the angular velocity and γ the ratio of specific heats, respectively. The first term of Eq. (11) refers to the change of the internal energy plus work done by pressure, and the fifth term represents the rate of energy transported across radius r by the viscous stress.

Recently, Ichimaru has developed a theory of magneto-hydrodynamic turbulence appropriate to plasmas in an accretion disk geometry and has derived the following formula for the viscous stress,[5)]

$$P_{r\varphi}=\frac{r}{2}\nu_T\frac{\partial\Omega}{\partial r}\,,\quad \nu_T=\left(\frac{2}{\pi}\right)^{3/2}\rho\left(\frac{kT}{m_H}\right)^{1/2}l\,, \tag{12}$$

where m_H is the proton mass and l the effective thickness of the disk. When the gas pressure P_g dominates the radiation pressure P_r, Eq. (12) reduces to

$$W_{r\varphi}=2\left(\frac{2}{\pi}\right)^{3/2}J(N)\,(1+N)^{1/2}\left(\frac{GM}{r^3}\right)^{-1/2}z_0P_{g0}\frac{r}{2}\frac{d\Omega}{dr}\,, \tag{13}$$

where

$$J(N)=\frac{(2N+2)!}{2^{2N+2}(N+1)!^2}\frac{\pi}{2}\,. \tag{14}$$

In deriving Eq. (13) the equation of state, $P_g=(2k/m_H)\rho T$, appropriate to a fully ionized hydrogen gas has been used, and the effective thickness l in Eq. (12) is put equal to z_0. When Keplerian motion prevails in the accretion disk, Eq. (13) can be written in a more simple form,

$$W_{r\varphi}=-\frac{3}{2}\left(\frac{2}{\pi}\right)^{3/2}(1+N)^{1/2}J(N)\,P_{g0}z_0 \quad \text{for} \quad P_{g0}\gg P_{r0}\,. \tag{15}$$

A number of attempts have been made to formulate the viscous stress in the theory of accretion disks. The essence of those theories is the α-model in which one assume the viscous stress to be proportional to the gas or radiation pressure, i.e., $P_{r\varphi}=-\alpha P_g$ or $P_{r\varphi}=-\alpha P_r$. The constant α has been believed to lie between 10^{-3} and 1. According to the α-model the integrated viscous stress can be written as

$$W_{r\varphi}=-2\alpha I(N+1)\,P_{g0}z_0\,. \tag{16}$$

Equations (15) and (16) give

$$\alpha=\frac{3}{4}\left(\frac{2}{\pi}\right)^{3/2}\frac{J(N)\,(1+N)^{1/2}}{I(N+1)}\,. \tag{17}$$

The viscous stress, Eq. (12), reduces to the α-model provided that the gas pressure dominates the radiation pressure and Keplerian motion prevails in the accretion disk. The constant α depends weakly on the polytropic index N and is nearly 2/3.

When the radiation pressure dominates the gas pressure the integrated viscous stress is written as

$$W_{r\varphi}=\left(\frac{2}{\pi}\right)^{3/2}(1+N)^{1/2}K(N)\,(P_{g0}P_{r0})^{1/2}\left(\frac{GM}{r}\right)^{-1/2}\left(\frac{z_0}{r}\right)r^2\frac{r}{2}\frac{d\Omega}{dr}\,, \tag{18}$$

where

$$K(N)=\sqrt{\pi}\,\Gamma(9(N+1)/8)/\Gamma(9(N+1)/8+1/2)\,. \tag{19}$$

If Keplerian angular velocity is assumed in Eq. (18), we have

$$W_{r\varphi}=-\frac{3}{4}\left(\frac{2}{\pi}\right)^{3/2}(1+N)^{1/2}K(N)\left(\frac{P_{g0}}{P_{r0}}\right)^{1/2}P_{r0}z_0 \quad \text{for} \quad P_{r0}>P_{g0}\,. \tag{20}$$

Equation (20) differs distinctly from the α-model, i.e., $W_{r\varphi}=-2\alpha I(N+1)P_{r0}z_0$. Comparing Eq. (20) with Eq. (16) one can see that the parameter α is proportional to the root of the ratio of pressures, $\sqrt{P_{g0}/P_{r0}}$, which is much smaller than unity, since $P_{g0}\ll P_{r0}$.

The explicit expression for the integrated energy loss rate E_R depends on whether the accretion disk is optically thick or not. For an optically thin disk E_R is given by the rate of free-free emission, $\varepsilon_{\mathrm{ff}}=\varepsilon_0\rho T^{1/2}$, integrated over the z-coordinate,

$$E_R=2\varepsilon_0 J(2N)\,\rho_0^2 T_0^{1/2}z_0\,, \tag{21}$$

where T_0 is the temperature at the equatorial plane.

In the optically thick limit E_R is given by outward energy flux across unit area of the disk surface,

$$E_R=-2\left(\frac{4acT^3}{3\kappa\rho}\frac{dT}{dz}\right)_{\mathrm{surface}}\,, \tag{22}$$

where κ is the opacity. If the radiation pressure dominates, Eq. (22) can be written as

$$E_R=2\frac{c}{\kappa}\frac{GM}{r^3}z_0\,, \tag{23}$$

since $P=aT^4/3$ then $(4/3)aT^3dT/dz=dP/dz=-GM\rho z_0/r^3$. In a gas pressure dominant disk Eq. (22) reduces to

$$E_R=\frac{16acT_0^4}{3\kappa\rho_0 z_0}[\xi(1-\xi^2)^{3-N}]_{\xi=1}\,, \tag{24}$$

where the opacity κ is assumed to be a constant. In order that Eq. (24) takes a finite and almost constant value near the surface layers of the disk, the polytropic index N must be 3 at these layers. This situation is quite analogous to the case of ordinary stellar surfaces. The emission rate is then given by

$$E_R=\frac{16}{3}\frac{acT_0^4}{\kappa\rho_0 z_0}\,. \tag{25}$$

§ 3. Optically thick and radiation pressure dominant accretion disk

In this and following chapters basic properties of accretion disks as well as their radial structures are inquired using the basic equations derived in § 2. In order to understand the essential features of accretion disks and especially to compare our result with those of other theories based on the standard accretion disk model, we have made the following simplification. (1) The radial velocity of disk matter is neglected compared with the azimuthal velocity and (2) the pressure gradient term in Eq. (9) is neglected compared with the gravity term. This simplification is equivalent to assume Keplerian motion for accretion disk matter, that is, Eq. (9) reduces to

$$v_\varphi=(GM/r)^{1/2}\,. \tag{26}$$

On the other hand, Eq. (10) can easily be integrated to give

$$\dot{M}rv_\varphi=-2\pi r^2 W_{r\varphi}+C\,. \tag{27}$$

The constant C refers to the rate at which angular momentum deposits in the central star when the disk surrounds a star such as a neutron star or a white dwarf. In the case of accretion onto a black hole we may take $r_1=6GM/c^2$ as the inner radius of Newtonian accretion disk. Since the motion of disk matter acquires a radial character irrespective of the transport of angular momentum at the domain inside r_1, we may put $W_{r\varphi}=0$ at $r=r_1$. Then, the constant C is determined as $\dot{M}(rv_\varphi)_{r=r_1}$. This can practically be neglected compared to other terms in Eq. (27) as far as sufficiently outer domains of the disk are concerned. In the following discussion we set $C=0$.

Eliminating $W_{r\varphi}$ in Eq. (11) with the aid of Eq. (27) we have

$$\dot{M}\frac{d}{dr}\left\{\frac{\gamma}{\gamma-1}\frac{W}{S}-\frac{3}{2}\frac{GM}{r}\right\}-2\pi rE_R=0\,. \tag{28}$$

In terms of Eqs. (5), (6) and (23), Eq. (28) can be rewritten as

$$\frac{d}{dr}\left(\frac{z_0}{r}\right)^2-\frac{1}{r}\left(\frac{z_0}{r}\right)^2+\frac{3}{2Ar}-\frac{4\pi c}{A\kappa\dot{M}}\left(\frac{z_0}{r}\right)=0\,, \tag{29}$$

where

$$A=\frac{\gamma}{\gamma-1}\frac{1}{2(N+1)}\frac{I(N+1)}{I(N)}\,. \tag{30}$$

Changing variables to the following non-dimensional ones,

$$y=\left(\frac{z_0}{r}\right),\quad x=\frac{4\pi c}{A\kappa\dot{M}}r\,, \tag{31}$$

Eq. (29) reduces to a simple differential equation,

$$\frac{dy^2}{dx}-\frac{y^2}{x}+\frac{3}{2A}\frac{1}{x}-y=0\,. \tag{32}$$

In deriving the above equation the opacity κ is assumed to be constant, that is, the opacity is assumed to be mainly due to electron scattering.

In the limit of geometrically thin disk configuration y^2 terms in Eq. (32) can be negligible, and the 0th order solution of Eq. (32) is $y=3/2Ax$. Evaluating the correction due to y^2 terms, y can be written as a power series of x,

$$y=\frac{3}{2Ax}-3\left(\frac{3}{2Ax}\right)^3+\cdots\,. \tag{33}$$

The first term of this solution refers just to the result derived from standard model calculation. The result of numerical calculation is shown in Fig. 1. In solving Eq. (32) the polytropic index is put tentatively to $N=3$ and the mass of the central black hole is taken to be $10M_{\odot}$. The dotted curve plots the first term in Eq. (33) and the solid curve (a) refers to a solution to Eq. (32) solved inward with a boundary condition $y=3/2Ax$ at $x\gg1$. The difference between these two curves is rather small in the domain $x>5$. Deviation is appreciable in the domain $x<5$, where y becomes larger than $1/2$, that is, the accretion disk expands considerably in the domain $x<5$.

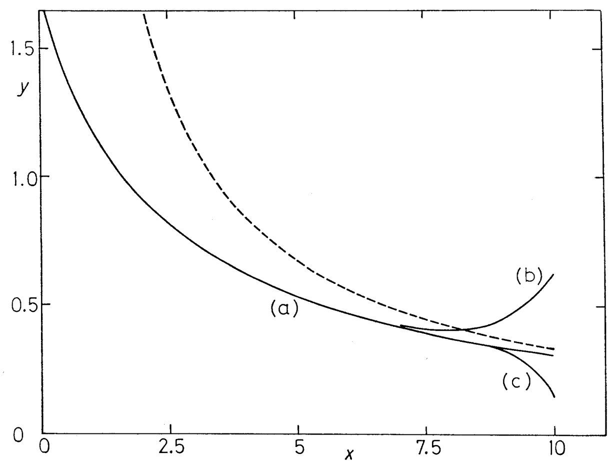

Fig. 1. Solutions of an optically thick and radiation pressure dominant accretion disk. The mass of the central black hole and the polytropic index are tentatively put to 10 $M_{\odot}$ and 3, respectively. Solid curves indicate solutions of Eq. (32) solved inward with different boundary conditions. The first term in Eq. (32) is plotted by the dashed curve.

The most remarkable behavior of solutions is shown in Fig. 1 by curves (b) and (c). The curve (b) plots y solved inward from $x=10$ with a boundary condition y_b which is chosen just twice the value given by the curve (a) at $x=10$. However, the solution quickly converges to the curve (a) as is shown in Fig. 1. The same is true for the curve (c) where a smaller value of y is imposed as the boundary condition. This behavior is easily understood when we examine the sign of the derivative, dy/dx. It takes a positive value in the domain above the locus, $y=(\sqrt{x^2+6/A}-x)/2$, which runs just above the curve (a). It takes a negative value in the domain below this curve. Consequently, any solution solved inward with an arbitrary boundary condition strongly converges toward a finite limiting value. This strong convergence has the happy consequence that two solutions fulfilling different outer boundary conditions approach the same solution at the inner domain of the disk.

The solution y combined with Eqs. (5), (20) and (27) determines disk parameters such as P_0, ρ_0, T_0 etc. After some tedious calculations, the disk parameters can be given by

$$P_0=P(N)\left(\frac{k}{m_H}\right)^{-4/9}\left(\frac{3}{a}\right)^{-1/9}\dot{M}^{8/9}\left(\frac{GM}{r}\right)^{8/9}r^{-16/9}, \tag{34}$$

$$\rho_0=2(1+N)P(N)\left(\frac{k}{m_H}\right)^{-4/9}\left(\frac{3}{a}\right)^{-1/9}\dot{M}^{8/9}\left(\frac{GM}{r}\right)^{-1/9}\left(\frac{z_0}{r}\right)^{-2}r^{-16/9}, \tag{35}$$

$$T_0=P(N)^{1/4}\left(\frac{k}{m_H}\right)^{-1/9}\left(\frac{3}{a}\right)^{2/9}\dot{M}^{2/9}\left(\frac{GM}{r}\right)^{2/9}r^{-4/9}, \tag{36}$$

where

$$P(N)=\left\{\frac{1}{6}\left(\frac{\pi}{2}\right)^{1/2}\frac{1}{(1+N)K(N)}\right\}^{8/9}. \tag{37}$$

The radial velocity of disk matter can be determined with the aid of Eqs. (8) and (35) as

$$v_r=\left\{\frac{1}{16\pi(1+N)^{3/2}I(N)P(N)^{9/8}}\right\}\left(\frac{P_{g0}}{P_0}\right)^{1/2}\left(\frac{z_0}{r}\right)^2 v_\varphi. \tag{38}$$

Since the bracketed term is of order 0.1 and, furthermore, $P_{g0}/P_{r0}<1$ holds in the radiation pressure dominant disk, the radial velocity can be shown to be negligibly small compared to the azimuthal velocity. This guarantees the assumption (1), made in the beginning of this chapter, through full domains of the radiation pressure dominant disk.

The above calculations can also be applied to the α-model. Since Eq. (32) has been derived irrespective of the viscous stress, the same thickness z_0 can be used to derive disk parameters appropriate to the α-model. The explicit formula for the viscous stress, $W_{r\varphi}=-2\alpha I(N+1)P_{r0}z_0$, is required when we wish to determine disk parameters. From Eqs. (5), (16) and (27), we have,

$$P_0=\frac{\dot{M}}{4\pi\alpha I(1+N)}\left(\frac{GM}{r}\right)^{1/2}\left(\frac{z_0}{r}\right)^{-1}r^{-2}, \tag{39}$$

$$\rho_0=\frac{(1+N)\dot{M}}{2\pi\alpha I(1+N)}\left(\frac{GM}{r}\right)^{-1/2}\left(\frac{z_0}{r}\right)^{-3}r^{-2}, \tag{40}$$

$$T_0=\frac{\dot{M}^{1/4}}{\{4\pi\alpha I(1+N)\}^{1/4}}\left(\frac{3}{a}\right)^{1/4}\left(\frac{GM}{r}\right)^{1/8}\left(\frac{z_0}{r}\right)^{-1/4}r^{-1/2}, \tag{41}$$

$$v_r = \frac{\alpha}{2(1+N)} \frac{I(N+1)}{I(N)} \left(\frac{z_0}{r}\right)^2 v_\varphi . \quad (42)$$

In terms of disk parameters derived above, we can examine domains in which the radiation pressure dominates the gas pressure and vice versa. In Fig. 2 the radial distance at the boundary between the radiation pressure dominated domain and the gas pressure dominated one is plotted as a function of the accretion rate. The radiation pressure dominates in the inner domain of the accretion disk. In further inner domain the difference of z_0 between our result and the standard model calculation becomes considerable as is seen from solutions plotted in Fig. 1. The hatched domain in Fig. 2 indicates that the deviation of z_0 from the standard model calculation amounts more than 20 %. In Fig. 2 we also plot the so-called critical accretion given by $\dot{M} = 24\pi GM/\kappa c$.

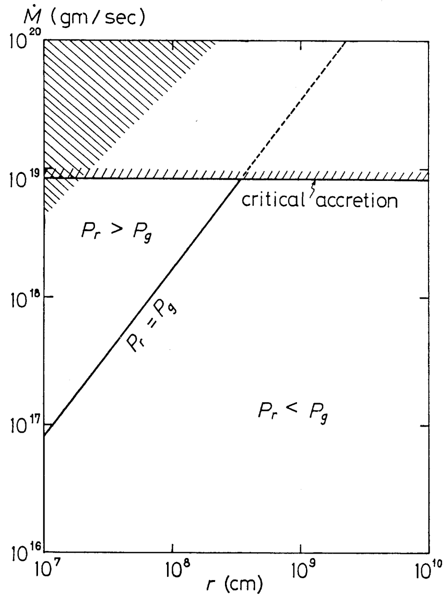

Fig. 2. The boundary at which the radiation pressure equals the gas pressure for an optically thick accretion disk. In the hatched domain the difference of z_0 between ours and standard model calculation amounts more than 20%.

§ 4. Optically thick and gas pressure dominant accretion disk

In a gas pressure dominant disk the viscous stress based on Eq. (12) reduces to the α-model, and one can determine α according to Eq. (17). Therefore, the result derived in this chapter can easily be applied to the α-model by slight modifications of equations. In terms of Eqs. (5) and (27) the energy loss rate, Eq. (25), can be written as

$$E_R = E_0 \dot{M}^{-1} \left(\frac{GM}{r}\right)^{9/2} \left(\frac{z_0}{r}\right)^{10} r \,, \quad (43)$$

where

$$E_0 = \frac{\pi ac}{3 \cdot 2^4} \frac{W_0}{\kappa} \frac{1}{(1+N)^5} \left(\frac{k}{m_H}\right)^{-4} \quad (44)$$

and

$$W_0 = \frac{3}{2} \left(\frac{2}{\pi}\right)^{3/2} (1+N)^{1/2} J(N) . \quad (45)$$

Inserting Eq. (43) into Eq. (28) and introducing non-dimensional variables $y = (z_0/r)$ and $x = (5\pi E_0 \dot{M}^{-2} (GM)^{7/2}/2)^{-2} r$, one can write the equation in a formula which includes only one parameter N as in Eq. (32). However, since x takes a value of order $10^{\sim 100}$ for relevant ranges of $\dot{M}$ and M, it is inconvenient to analyse the accretion disk with these variables.

The best way is to introduce the following non-dimensional variables,

$$x = \frac{r}{r_1} = \left(\frac{c^2}{6GM}\right) r\,, \quad y = b\left(\frac{z_0}{r}\right), \tag{46}$$

where

$$b = \left\{\frac{2\pi E_0}{A}\dot{M}^{-2}\left(\frac{6GM}{c^2}\right)^3\left(\frac{c^2}{6}\right)^{7/2}\right\}^{1/8}, \tag{47}$$

and A was defined in Eq. (30). The basic equation is then given by

$$\frac{dy^2}{dx} - \frac{y^2}{x} + \frac{B}{x} - \frac{y^{10}}{x^{3/2}} = 0\,, \tag{48}$$

where

$$B = \frac{3b^2}{2A}\,.$$

Since B is $\sim 10^5$ in relevant ranges of $\dot{M}$ and M, a special solution of Eq. (48) can be approximated as

$$y = (B^2 x)^{1/20} - \frac{9}{100}\frac{1}{B}(B^2 x)^{3/20} + \cdots\,. \tag{49}$$

In practice, the second term and also higher terms are almost completely negligible. Therefore, the solution reduces to the standard model calculation. In fact, numerical calculation shows that a solution with the boundary condition, $y_b = (B^2 x)^{1/20}$ at $x \gg 1$, runs closely along $y = (B^2 x)^{1/20}$. The strong convergence character of solutions toward a limiting value has also preserved in the gas pressure dominant accretion disk. Furthermore, the y^{10} term in Eq. (48) gives rise to a more strong convergence character than that of the radiation pressure dominant accretion disk.

Disk parameters can be written by means of Eqs. (5), (15) and (27) as

$$P_{g0} = \frac{1}{2\pi W_0}\dot{M}\left(\frac{GM}{r}\right)^{1/2}\left(\frac{z_0}{r}\right)^{-1} r^{-2}\,, \tag{50}$$

$$\rho_0 = \frac{(1+N)}{\pi W_0}\dot{M}\left(\frac{GM}{r}\right)^{-1/2}\left(\frac{z_0}{r}\right)^{-3} r^{-2}\,, \tag{51}$$

$$T_0 = \frac{1}{4(1+N)}\left(\frac{m_H}{k}\right)\left(\frac{GM}{r}\right)\left(\frac{z_0}{r}\right)^2, \tag{52}$$

$$v_r = \frac{W_0}{4(1+N)I(N)}\left(\frac{z_0}{r}\right)^2 v_\varphi\,. \tag{53}$$

In Eqs. (50)$\sim$(53) if we replace W_0 by $2\alpha I(N+1)$, the result reduces to the well-known α-model.

§ 5. Optically thin accretion disk

Calculations are the same as the case of the gas pressure dominant disk. The energy loss rate can be written as

$$E_R = E_0 \dot{M}^2 \left(\frac{GM}{r}\right)^{-1/2} \left(\frac{z_0}{r}\right)^{-4} r^{-3}, \tag{54}$$

where

$$E_0 = \frac{\varepsilon_0 J(2N)\,(1+N)^{3/2}}{\pi^2} W_0^{-2} \left(\frac{m_H}{k}\right)^{1/2} \tag{55}$$

and W_0 has been given in Eq. (45). Inserting Eq. (54) into Eq. (28) and making use of non-dimensional variables

$$x = \left(\frac{c^2}{6GM}\right) r, \quad y = b\left(\frac{z_0}{r}\right) \tag{56}$$

with

$$b = \left\{\frac{A}{2\pi}(E_0 \dot{M})^{-1} \left(\frac{6GM}{c^2}\right) \left(\frac{c^2}{6}\right)^{3/2}\right\}^{1/6}, \tag{57}$$

we have

$$\frac{dy^2}{dx} - \frac{y^2}{x} + \frac{B}{x} - \frac{1}{x^{1/2} y^4} = 0, \tag{58}$$

where

$$B = \frac{3b^2}{2A}. \tag{59}$$

Now, let us examine the locus of zero-derivative, $dy/dx = 0$, which is given from Eq. (58) by

$$y^8 (B - y^2)^2 - x = 0. \tag{60}$$

This locus is plotted in Fig. 3 by a thin solid curve, which splits the figure into two domains. In the middle domain the derivative is negative, while in the outer domain surrounding the middle domain it takes a positive value. It is to be noticed that the existence of these two domains is responsible to bimodal behavior of an optically thin accretion disk. Ichimaru has first found bimodal behavior for an optically thin disk. Further, he has argued implication between the bimodal behavior found in an optically thin disk surrounding a black hole and alternative high and low luminosity states observed in the X-ray source Cyg X-1.[7]

In Fig. 3 three typical solutions for Eq. (58) are plotted by thick solid curves, where we have tentatively assumed the outer boundary of the disk to be

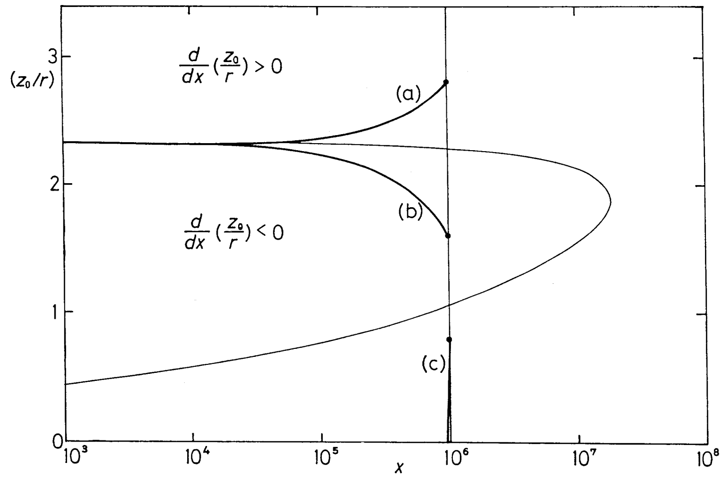

Fig. 3. Solutions of an optically thin accretion disk. The mass of the black hole and the accretion rate are assumed to be $10\,M_\odot$ and 10^{17} gm/sec, respectively, and the polytropic index is also taken to be 3. The locus which gives the zero derivative is plotted by the thin solid curve. Solutions of Eq. (58) are indicated by thick solid curves.

$r_b = 10^{13}$cm. This value may somewhat be large as compared to estimate from the size of Roche lobe in X-ray binary systems. But the essential feature of solutions preserves if r_b is smaller than 10^{14}cm or $x<10^7$. Let us denote two solutions to Eq. (60) by $y_{\rm max}$ and $y_{\rm min}$ ($<y_{\rm max}$). Then, solutions of Eq. (58) are divided into two families depending on whether the boundary value of y is larger than $y_{\rm min}$ or not. Solutions designated by (a) and (b) in Fig. 3, which start with boundary conditions larger than $y_{\rm min}$, converge to the limiting value $y_{\rm max}$. On the contrary if we begin with a smaller boundary value than $y_{\rm min}$, the thickness y of the disk decreases steeply as we proceed inward. As y decreases the optical thickness of the disk increases since the density is proportional to y^{-3}. Consequently, the disk changes gradually to an optically thick and gas pressure dominant disk configuration.

Whether accreting matter evolves into an optically thin disk or an optically thick disk, depends on the thickness y_b at the boundary. If $y_b > y_{\rm min}$ accreting matter evolves into an optically thin disk, while an optically thick disk is formed if $y_b < y_{\rm min}$. We can rewrite this condition with a more appropriate expression by means of the temperature at the boundary. Before describing the condition we note that disk parameters for an optically thin accretion disk are given by Eqs. (50)$\sim$(53). In terms of Eq. (52) the condition is written as

$$\frac{T_b}{T_{\rm crit}}\begin{cases} >1\,, & \text{(an optically thin disk)} \\ <1\,, & \text{(an optically thick disk)} \end{cases} \tag{61}$$

where

$$T_{\rm crit}=\frac{1}{4(1+N)}\left(\frac{m_H}{k}\right)\left(\frac{GM}{r_b}\right)\left(\frac{z_0}{r}\right)^2_{\rm min}. \tag{62}$$

Suppose that accreting matter travels adiabatically from the Roche surface to the disk boundary in a binary X-ray source. Then, the temperature of accreting matter rises to

$$T_g=\frac{m_H}{3k}\left(\frac{GM}{r_b}\right), \tag{63}$$

at the disk boundary. In terms of this T_g, Eq. (62) is written as

$$T_{\rm crit}=\left\{\frac{3}{4(1+N)}\left(\frac{z_0}{r}\right)^2_{\rm min}\right\}T_g. \tag{64}$$

Since $(z_0/r)_{\rm min}(=y_{\rm min}/b)$ is smaller than unity for $x<10^6$, $T_{\rm crit}$ becomes smaller than T_g. This means that in order for accreting matter to evolve into an optically thick disk configuration energy loss process must operate effectively to decrease the temperature below $T_{\rm crit}$ at the boundary. Otherwise, accreting matter evolves into an optically thin disk configuration.

§ 6. Concluding remarks

We have, so far, examined radial structures of accretion disks by means of basic equations we have developed in § 2. We find that the radial structure of an optically thick disk converges, irrespective of the outer boundary condition, to the limiting value given by the standard model calculation. However, in the radiation pressure dominant disk with a relatively intense $\dot{M}$ the difference of the structure is appreciable between our calculation and the standard model calculation.

On the other hand, the optically thin accretion disk shows in particular bimodal behavior as has been discussed in § 5. The implication between such bimodal behavior and the observed nature of galactic X-ray sources has not been discussed in this paper. As has been proposed by Ichimaru, such a bimodal transition may produce alternative high and low luminosity states observed in Cyg X-1. The bimodal behavior also predicts that there exists X-ray sourses which always stay in the optically thin state or the optically thick state. The famous X-ray source, Sco X-1, may always stay in the optically thin state.

We are interested in the structure of an geometrically thick accretion disk. The optically thin disk and the optically thick and radiation pressure dominant disk with a relatively large $\dot{M}$ fall to this category. In geometrically thick accretion disks the azimuthal velocity cannot be approximated by Keplerian velocity. In terms of Eq. (50) we can calculate the pressure gradient term in Eq. (9) and the azimuthal velocity is modified as

$$v_\varphi=\left\{1-\frac{3}{4}\frac{I(N+1)}{I(N)(N+1)}\left(\frac{z_0}{r}\right)^2\right\}^{1/2}\left(\frac{GM}{r}\right)^{1/2}. \tag{65}$$

One can see that as z_0/r increases v_φ decreases according to Eq. (65). The disk approaches such a configuration that gravity due to the central star balances the pressure gradient force, instead of the centrifugal force. The structure may distinctly differ from the standard model calculation.

References

1) J. E. Pringle and M. J. Rees, Astron. and Astrophys. **21** (1972), 1.
2) N. I. Shakura and R. A. Sunyaev, Astron. and Astrophys. **24** (1973), 337.
3) I. D. Novikov and K. S. Thorne, *in Black Hole*, edited by C. DeWitt and B. DeWitt (Gordon and Breach, New York, 1973).
N. Shibazaki and R. Hōshi, Prog. Theor. Phys. **54** (1975), 706.
K. S. Thorne and R. H. Price, Astrophys. J. **195** (1975), L101.
D. M. Eardley and A. P. Lightman, Astrophys. J. **199** (1975), L153.
4) A. P. Lightman and D. M. Eardley, Astrophys. J. **187** (1974), L1.
J. E. Pringle, M. J. Rees and A. G. Pacholczyk, Astron. and Astrophys. **29** (1973), 179.
N. I. Shakura and R. A. Sunyaev, Month. Notices Roy. Astron. Soc. **175** (1976), 613.
5) S. Ichimaru, Astrophys. J. **208** (1976), 701.
6) S. Ichimaru, Astrophys. J. **214** (1977), 840.
7) H. Tananbaum, H. Gursky, E. Kellogg and R. Giacconi, Astrophys. J. **177** (1972), L5.
J. Heise, A. Brinkman, J. Schrijver, R. Mewe, A. den Boggende, E. Gronenschild, D. Parsignault, J. Grindley, H. Schnopper, E. Schreier and H. Gursky, Nature **256** (1975), 107.